Journal of Mechanical Engineering and Sciences
ISSN (Print): 2289-4659; e-ISSN: 2231-8380
Volume 13, Issue 3, pp. 5390-5406, September 2019

DOI: https://doi.org/10.15282/jmes.13.3.2019.12.0438

Failure study of the woven composite material: 2.5 D carbon fabric/ resin epoxy

Abderraouf Gherissi

Mechanical Engineering Department, College of Engineering,
University of Tabuk, P.O.Box : 741, Tabuk 71491, Saudi Arabia.
Laboratoire de Mecanique, Productique et Energétique (LMPE), ENSIT,
Université de Tunis - Tunisia, 5 Avenue Taha Hussein, BP, 56, Bâb Manara, 1008 Tunisia.
*Email: gherissi.abderraouf@gmail.com / a.gresi@ut.edu.sa
Phone: +21656351977 / +966543440530

ABSTRACT

In this paper, an experimental analysis of the failure of a single layer woven fabric composite 2.5 D G1151/ Resin Epoxy, through a tensile test at 0°, 45° and 90° is investigated. In addition, an FE simulation of failure were elaborated through multiscale modeling method, a micro, then meso and macro scale. The microscale simulation was elaborated on the ABAQUS standard simulation of a 3D unit cell of random fibers' distribution of a single yarn. The meso scale simulation developed in MATLAB. The meso approach was based on the extraction behaviour of Representative Volume Elementary (RVE) of the 2.5 D woven composite. The macroscale simulation was elaborated on the ABAQUS standard simulation. With reference to the numerical and experimental study, the results show a good agreement. The present investigation is an important preliminary study in the process forming of single woven carbon 2.5 D composite.

Keywords: Composite failure; FE modelling; multiscale approach; woven carbon fabric G1151/resin epoxy.

INTRODUCTION

In the last years, the woven composite materials have attracted much interest of researchers, aircraft and aerospace industries. The woven fibers reinforcement allows an easier lay-up for complex surfaces, lightweight, great mechanical performance and excellent formability. To properly explore woven composite materials, several recent numerical, analytical and experimental investigations were carried out. Some studies were investigated in using multiscale modelling approaches [1-5], while others studied the forming processes of woven fabric reinforced composites [6-8]. The numerical application of the deep drawing of 2.5 D woven fabrics was developed in the study of Gherissi et al. [7]. The hierarchical modelling techniques were investigated by Naoki et al. [8]. While other researchers conducted more in depth investigations into the damage and failure modes [9-11]. The failure modes can be investigated separately, and generally arise together (e.g.: matrix cracking and delamination) [9]. To solve the problems of modelling woven composite's failure, the finite element method (FEM) was adopted by several authors because of its simplicity and efficiency [9-12]. In the

same field, the study of T. Okabe et al [10] reproduced the damage process in composite with a non-uniform fiber arrangement, based to the work of Hobbiebrunken et al [11]. As well, to predict the mechanical behaviour and damage response of composite laminates, Ganesh Soni et al [12] developed a three-dimensional multi-fibre multi-layer micromechanical finite element model, while, S.D. Green et al [13] compared failure results produced using idealised geometry with realistic geometry obtained from detailed simulation of the preform during weaving and compaction of 3D woven composite. Moreover, Kyle C. Warren et al [14] developed a three-dimensional progressive damage model to capture the onset and initial propagation of damage within a three-dimensional woven composite in a single-bolt, double-shear joint.

Several studies builded the study based to Hashin's failure criteria [15] and the Matzen millere et al [16] damage model. In the present work, the experimental study was developed to evaluate the single layer woven composite material behaviour. A microscale modelling simulation for the composite G1151/Resin Epoxy based to the previous work [17] was carried out. The microscale result was integrated in meso-macro scale FEM approach. To predict the onset and initial propagation of damage by using Hashin's failure criteria, a macro simulation under ABQUS was carried out. To validate the multiscale model a comparison between numerical model for prediction failure response and the tensile test experimental results on G1151/Resin Epoxy was carried out.

MATERIAL AND EXPERIMENT

The experimental part focuses in the determination of the behaviour of a specimen of 2.5D woven composite material. The damage initiation and propagation under uniaxial tensile test was analysed. The material degradation is experienced in tensile and it was investigated in several previous works [13, 14, 18]. For the present experimental work, the characterization of the composite was included tension, on 0°, 90° and 45°. The specimen preparation was conducted according to the standard ASTM D 3039 [19]. All samples were cut up according to the Figure 1. The experiments conducted for five specimens per test. All tests were carried out on tensile test machine Zwik/Roell, 10 kN as shown in Figure 2(a). An example of failure of specimen after tensile test showed the change in orientation of yarns is shown in Figure 2(b).

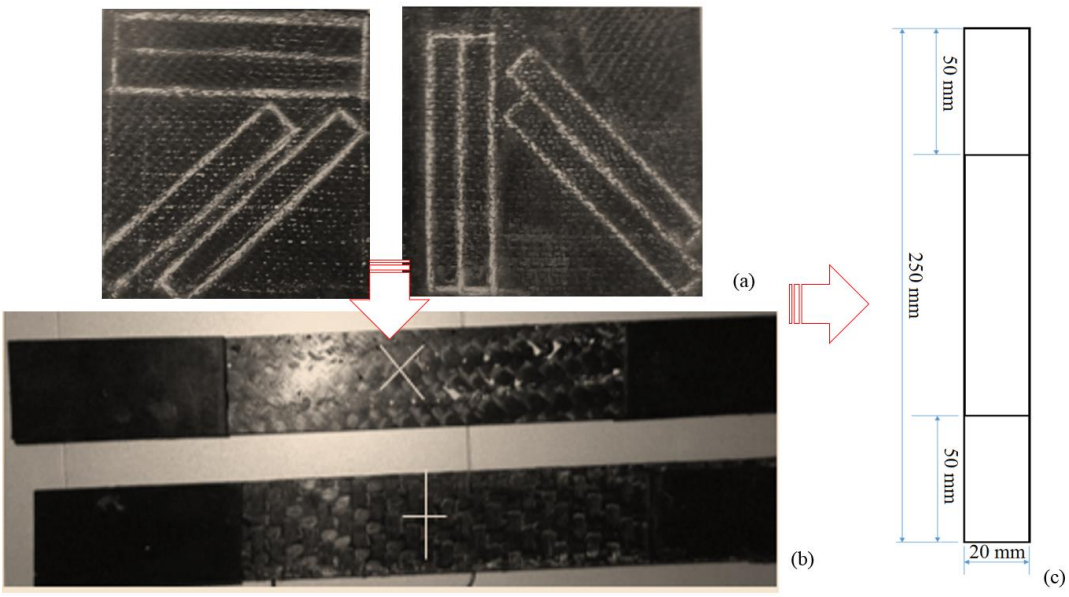

Figure 1. Specimens preparation for the tensile test: (a) Composite plate, (b) cut at 0°, 90° and 45° and (c) specimen dimensions.

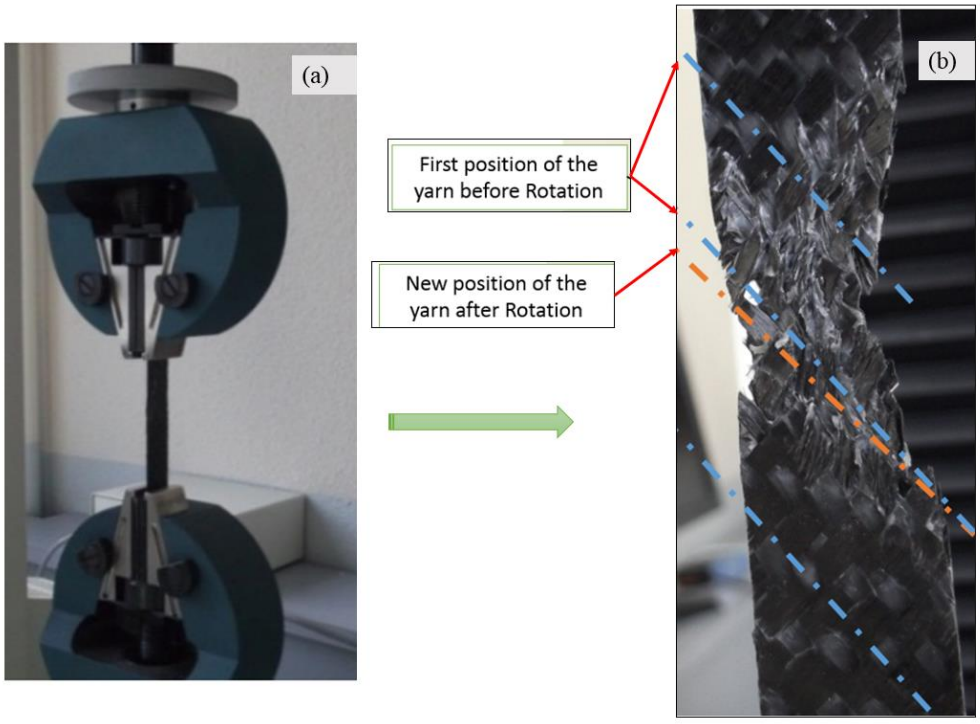

Figure 2. The specimen G1151/Resin Epoxy mounted in the tensile test machine Zwik/Roell, 10 kN.

The experimental results of the tensile test at 0° and 90° are shown in the Figure 3. It is observed that there is a small difference between the two main directions of weaving of the composite. In Figure 4 the bias test shows a weak behaviour compared with two main directions at 0° and 90°.

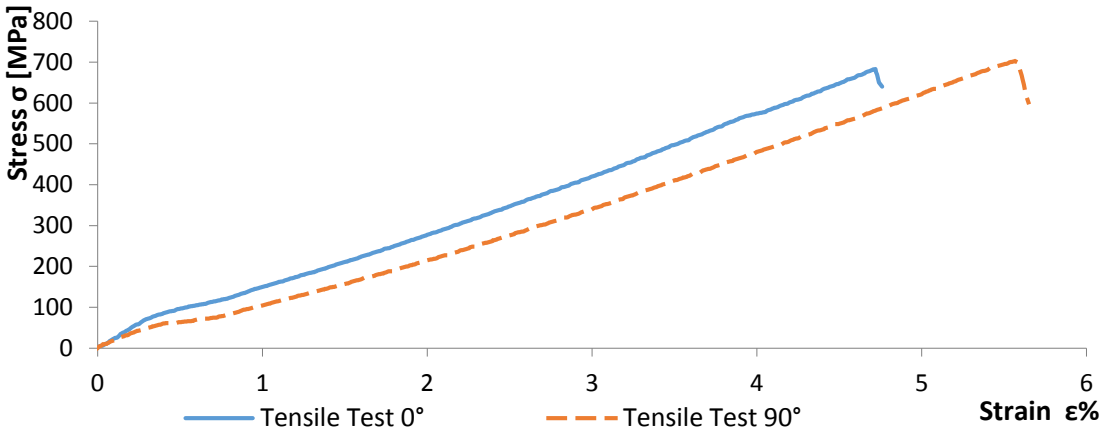

Figure 3. Tensile Test curve at 0° and 90°.

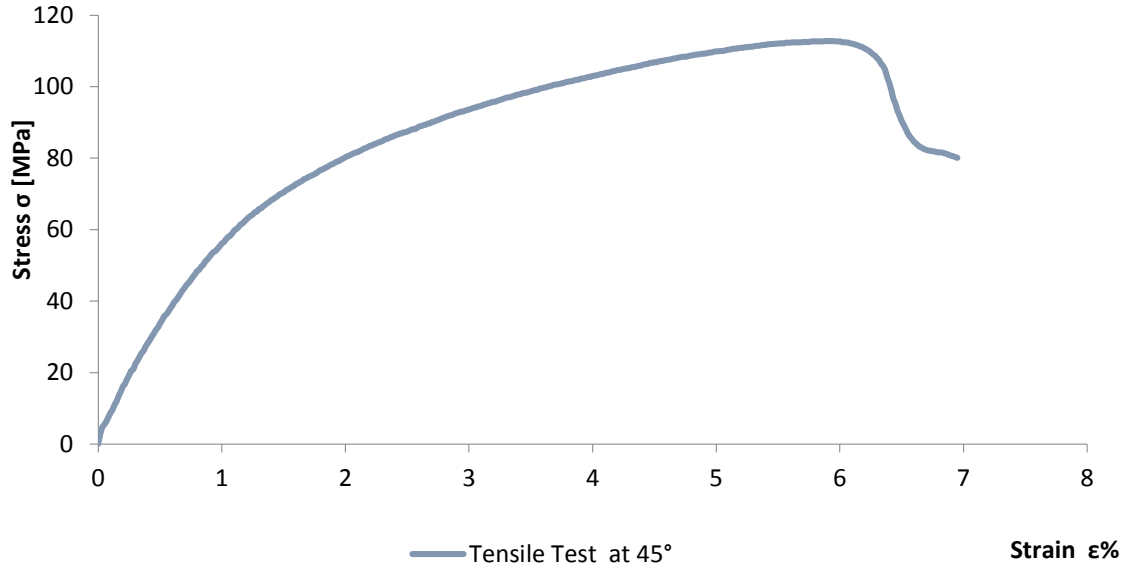

Figure 4. Tensile Test Curve at 45°.

According to ASTM D3039 [19] the tensile Chord Modulus of Elasticity E chord could be calculated by the Equation (1) and the Poisson's Ratio by Chord method by the Equation (2):

$$E^{chord} = \frac{\Delta\sigma}{\Delta\varepsilon} \tag{1}$$

Where: $\Delta\sigma, \Delta\varepsilon$ are respectively the difference in applied tensile stress between the two strain points, MPa; and the difference between the two strain points (nominally 0.002).

$$\nu = \frac{\Delta\varepsilon_t}{\Delta\varepsilon_l} \tag{2}$$

Where: $\Delta\varepsilon_t, \Delta\varepsilon_l$ are respectively the difference in lateral strain between the two longitudinal strain points; and the difference between the two longitudinal strain points (nominally 0.001, 0.002, or 0.005). According to ASTM D3039 [19] the standard deviation for each series of tests and the coefficient of variation for each property are determined by the following Equation (3-5):

$$CV = \frac{100 * S_{n-1}}{\overline{x}} \tag{3}$$

where,
$$S_{n-1} = \sqrt{\frac{(\sum_{i=1}^{n} x_i^2 - nx^{-2})}{(n-1)}} \tag{4}$$

and,
$$\overline{x} = \frac{(\sum_{i=1}^{n} x_i)}{n} \tag{5}$$

where, n number of specimens, xi measured property, $\overline{x}$ sample average, CV coefficient of variation in percent (%) and S_{n-1} : standard deviation. The tensile properties of the Uni-ply Resin Epoxy / G1151 are presented in the Table 1.

Table1. Experimental Uni-ply tensile properties vf = 50%.

Ultimate Tensile Strength (MPa)	0°	683	(6%)
	45°	113	(8%)
	90°	700	(5%)
Tensile Modulus (MPa)	0°	24000	(2%)
	45°	6780	(9%)
	90°	15500	(2%)
Poisson's Ratio	ν_{12}	0.23	(2%)

The experimental results show that in the two main directions (0°, 90°) the provide properties are more resistant than the 45° directional composite. However, the tensile strength and modulus of a single woven fabric composite are lower than those of multi layered laminates composite presented in the literature. The principal reason for their lower tensile properties is the presence of fiber undulation in woven fabrics as the G1151 fiber yarns in the weft direction cross over and under the fiber yarns in the warp direction to create an inter locked structure. Under tensile loading, these wavy fibers tend to be straight, which generates high stresses in the resin. As a consequence, micro-cracks are formed in the resin at quite low loads. Then the G1151 fibers in woven fabrics are subjected to additional mechanical handling during the weaving process, which tends to reduce their tensile strength.

THE THEORETICAL BEHAVIOR OF THE COMPOSITE

The analysis of woven fabric lamina requires a description of the architecture geometry of the fabric [20-23]. The periodicity of woven-fibre composites and the isolation of a repeating woven unit-cell allow the construction of analytical micromechanical model. The geometric description of the meso RVE include yarn's width, thickness and path for an undulating yarn. Also there are several models gives an overall composite properties based to rule of mixture, so the relative unidirectional elastic behaviour are calculated as written in Equation 6:

$$\mathrm{E_1} = \mathrm{E_f V_f} + \mathrm{E_m V_m} = \mathrm{E_f V_f} + \mathrm{E_m}\left(1 - \mathrm{V_f}\right) \tag{6}$$

The Halpin-Tsai model for transverse modulus gives the Equation 7:

$$E_2 = \frac{E_m\left(1 + \xi\eta_1 V_f\right)}{\left(1 - \eta_1 V_f\right)} \tag{7}$$

where,

$$\eta_1 = \frac{\left(E_f - E_m\right)}{\left(E_f + \xi E_m\right)}$$

The Halpin-Tsai equations are applicable to shear modulus, giving the preferred Equation (8):

$$G_{12} = \frac{G_m\left(1 + \xi\eta_2 V_f\right)}{\left(1 - \eta_2 V_f\right)} \tag{8}$$

where,

$$\eta_2 = \frac{\left(G_f - G_m\right)}{\left(G_f + \xi G_m\right)}$$

The parameter ξ is adjustable, but is usually close to unity as shown in Equation (9).

$$\mathrm{G_{23}} = \frac{\mathrm{E_2}}{2\left(1 + \nu_{23}\right)} \tag{9}$$

For Poisson's ratio, the Equation (10):

$$\nu_{12} = \nu_{\mathrm{f}} \mathrm{V_f} + \nu_{\mathrm{m}} \mathrm{V_m} \tag{10}$$

According to the work of Hull and Clyne H. X. Zhu et al [24] gives the following expression for the other out-of-plane Poisson's ratio in terms of the bulk modulus (K) (see Equation (11)):

$$\nu_{23} = 1 - \nu_{12} - \frac{E_2}{3K} \tag{11}$$

where,

$$\frac{1}{\mathrm{K}} = \frac{\mathrm{V_f}}{\mathrm{K_f}} + \frac{\mathrm{V_m}}{\mathrm{K_m}}$$

with,

$$K_f = \frac{E_f}{3(1-2\nu_f)}$$

And,

$$K_m = \frac{E_m}{3(1-2\nu_m)}$$

Also several authors [25-32] estimate the macro woven fabric composite behaviour as elastic. The behaviour could be written as follow, Equation (12-17):

$$\left(\frac{2}{E_1}\frac{E_1\left(E_1+(1-\nu_{12}^2)E_2\right)-\nu_{12}^2E_2^2}{E_1\left(E_1+2E_2\right)+(1+2\nu_{12}^2)E_2^2}\right)^{UD}=\left(\frac{1}{E_1}\right)^{WF} \tag{12}$$

$$\left(\frac{4}{E_1}\frac{\nu_{12}E_2(E_1-\nu_{12}^2E_2)}{E_1\left(E_1+2E_2\right)+(1+2\nu_{12}^2)E_2^2}\right)^{UD}=\left(\frac{\nu_{12}}{E_1}\right)^{WF} \tag{13}$$

$$\left(\frac{1}{E_1}\frac{E_1(\nu_{12}+\nu_{23}+\nu_{12}\nu_{23})+\nu_{12}^2E_2)}{E_1+(1+2\nu_{12})E_2}\right)^{UD}=\left(\frac{\nu_{13}}{E_1}\right)^{WF} \tag{14}$$

$$\left(\frac{(1-\nu_{23}^2)E_1^2+(1+2\nu_{12}+2\nu_{12}\nu_{23})E_1E_2-\nu_{12}^2E_2^2)}{E_1E_2(E_1+(1+2\nu_{12})E_2)}\right)^{UD}=\left(\frac{1}{E_3}\right)^{WF} \tag{15}$$

$$\left(\frac{1}{G_{12}}\right)^{UD}=\left(\frac{1}{G_{12}}\right)^{WF} \tag{16}$$

$$\left(\frac{1+\nu_{23}}{E_2}+\frac{1}{2G_{12}}\right)^{UD}=\left(\frac{1}{G_{13}}\right)^{WF} \tag{17}$$

where, $(E_1)^{WF}=(E_2)^{WF}$ and $(\nu_{13})^{WF}=(\nu_{23})^{WF}$.

Then the analytic elastic properties of the macro scale behaviour of the woven fabric G1151/Resin Epoxy could be calculated and are listed in the Table 2:

Table 2. Analytic elastic properties of the woven fabric composite G1151/Resin.

E1(MPa) E2(MPa)	E3(MPa)	G12(MPa)	G23(MPa)
106281	14281	3975	4400
G13(MPa)	ν12	ν23	ν13
4400	0.457	0.404	0.404

Material Microstructure and Microscale Modelling Approach

The fabric utilized in this study was a 2.5 D woven interlock G1151 from Hexcel® Company. The microscale modelling of the fabric were essentially based to the choice of the RVE. The 3D random RVE is a cubic shape, it was established based to several studies [17, 18]. The RVE should have the smallest size which makes it representative of the yarn of the woven composites. Then it was selected a RVE, it is a random unit cell (see Figure 5). The volumetric fraction of the reinforcement is calculated by the report between the volume of the fibers and the total volume of the basic cell. To choose the optimum size of RVE, it was necessary to satisfy the following criteria: firstly, the RVE must be small enough to represent the microscopic structure of material. Secondly, the RVE must sufficiently large to describe the overall behaviour of the material. And thirdly, the material properties must be independent of the location of the selected unit cell wherever it is taken. For that reason, a statistical study was carried out to identify the random RVE of the yarn. The idea was to vary the size and the position of the RVE on the micrograph see Figure 5.

The elastic behaviour of the Resin Epoxy/ G1151 fiber is calculated by periodic homogenization method via a simulation in finite element method (FEM) developed using ABAQUS software for the 3D random RVE. The simulation and calculation of the stiffness coefficients $C_{ijkl}^{\hom}$ of the random 3D RVE it was constructed by imposing macroscopic displacement and shears to the unit cell. For i =j=k=l ; i, j, k, l $\in$ {1,2,3}, the $C_{ijkl}^{\hom}$ coefficients, is determined by imposing a small displacement on the three main directions of the RVE, that correspond with the symmetry's axes of the cell; and for i =k and j=l i, k $\in$ {1, 2} and j, l $\in$ {2, 3}, the coefficients $C_{ijkl}^{\hom}$ are determined by imposing to the basic cell a simple shear displacement. In order to apply the FEM, it was necessary to fix the appropriate boundary conditions to the RVE for each type of load, this method has been adopted by several authors [17, 18]. The results of microscale simulation of the 3D random unit cell of G1151/Epoxy are shown in Table 2.

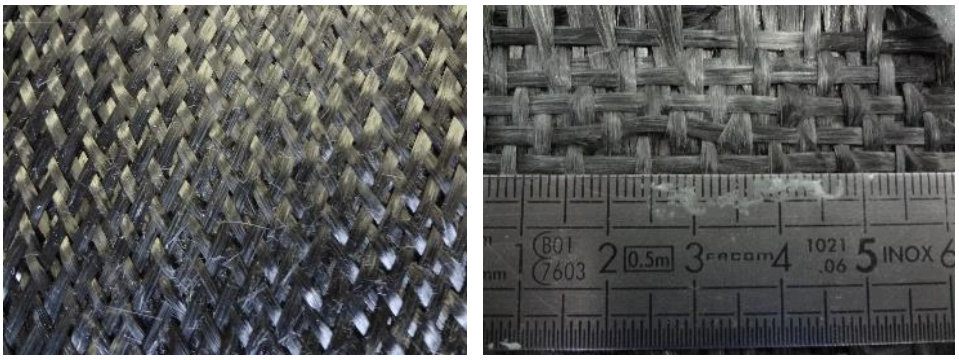

Woven fabric G1151

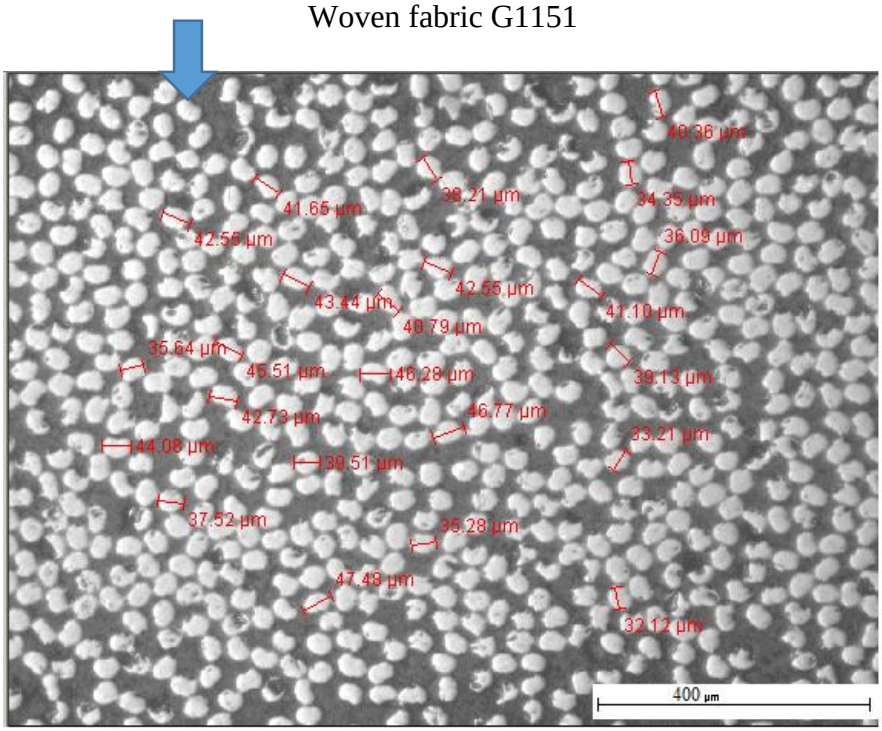

(a)

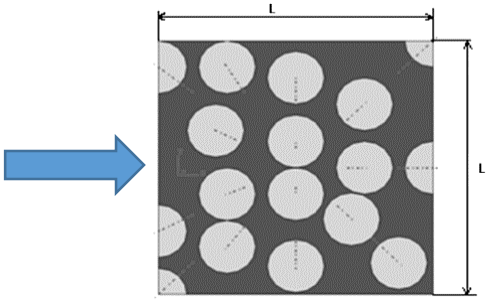

(b)

Figure 5. (a) The G1151/Resin Epoxy microstructure and (b) random RVE of the yarn.

Table 3. Microscale results for 3D random unit cell of G1151/Epoxy

Parameters	Value
E_X (GPa)	183
E_Y (GPa)	11.6
E_Z (GPa)	10
ν_{XY}	0,10
ν_{XZ}	0,22
ν_{YZ}	0,24
G_{YZ} (MPa)	4498
G_{XZ} (MPa)	5354
G_{XY} (MPa)	5369

The Meso Scale Approach

The purpose of this section is to implement the results already obtained from the random micro scale modelling approach in an FEM calculation program developed on MATLAB software. The programme resolve all problems associated to woven fabric composites, such as yarn's orientations, weft and warp intersection and interpenetration, meshing and complex meso structure FE simulation, the details and the approach stood in the previous work of GHERISSI.A et al [7]. To resolve the case of woven fabric G1151 unit cell carbon fibers and resin epoxy it was necessary to assuming that the rotation of yarns during the tensile test at room temperature is blocked by the matrix then the rotation of yarns is so much feeble for bias and negligible for 0 and 90° tensile tests. Then this assumption gives two cases of predefined orientation of the unit cell (see Figure 6). First, test at 0 or 90°, in this case during the tensile test, the fabric keeped a fixe position without any changes in fabric's angle. Second, test at 45°, in this case the fabric position is mainly inflienced by the type of fabric and matrix and the resin epoxy matrix. The limitation of movement in the fabric is provoked by resin, but the fabric's angles will not be keeped the same during the tensile test, so it was assumed that small reorientation will occurs to the fabric due to bias tensile force (see Figure 6). The results of meso simulation of RVE is presented in the Table 4.

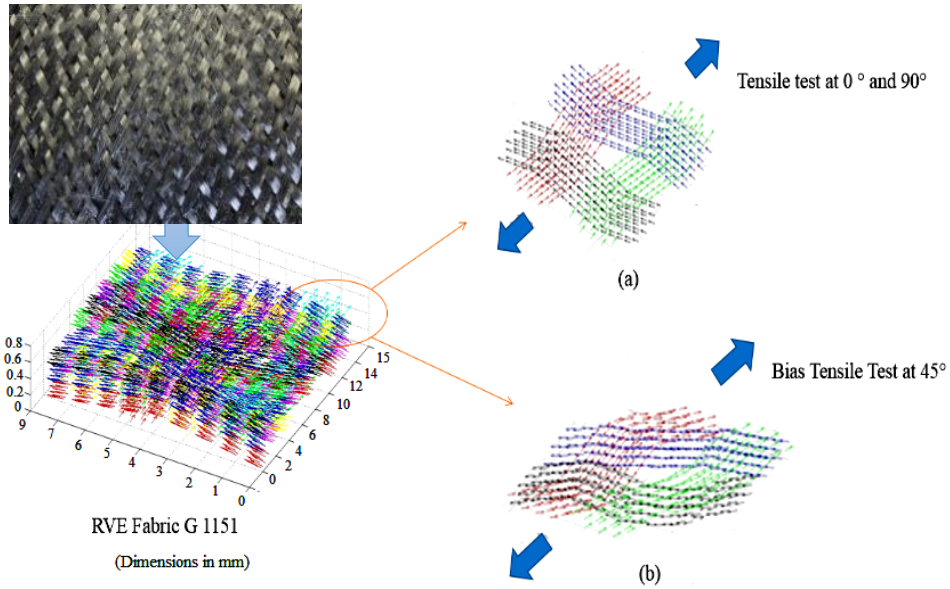

Figure 6. The orientation of the Meso RVE of the G1151 during the tensile test: (a) case of 0 and 90 test and (b) case of 45° test.

According to the regrouped results shown in the Table 2 it is observed that the bias tensile test on RVE orientation at 45° gives less elastic behaviour compared with the normal RVE, orientation at 0 and 90°.

Table 4. Meso scale simulation results of the Resin Epoxy/G1151 carbon fibers.

Direction of loaded fabrics	0°-90°	45°
E_X (MPa)	65284	19962
E_Y (MPa)	122410	28327
E_Z (MPa)	43108	2154.2
ν_{XY}	0.0084	0.0034
ν_{XZ}	0.9231	0.0187
ν_{YZ}	0.8289	0.0249
G_{YZ} (MPa)	8122.7	2649.2
G_{XZ} (MPa)	10019	1888.5
G_{XY} (MPa)	4326.6	21332

Macro FE Simulation of Failure On G1151/Resin Epoxy

To evaluate different failure mode acts together in composite G1151/Resin Epoxy, the failure criteria of Hashin's [15] was used. Hashin's criteria are implemented within two dimensional classical lamination approach for point stress calculations with ply discounting as the material degradation model. Failure indices for Hashin's criteria are related to fibre and

matrix failures and involve four failure modes. The criteria are extended to three dimensional problems where the maximum stress criteria are used for transverse normal stress component. The failure modes included in Hashin's criteria are six, listed as follows in Equation (18-23) [15]:

First, tensile fibre failure for $\sigma_{11} \geq 0$

$$\left(\frac{\sigma_{11}}{X_T}\right)^2 + \frac{\sigma_{12}^2 + \sigma_{13}^2}{S_{12}^2} = \begin{cases} \geq 1 & \text{failure} \\ < 1 & \text{no failure} \end{cases} \tag{18}$$

Second, compressive fibre failure for $\sigma_{11} < 0$

$$\left(\frac{\sigma_{11}}{X_C}\right)^2 = \begin{cases} \geq 1 & \text{failure} \\ < 1 & \text{no failure} \end{cases} \tag{19}$$

Third, tensile matrix failure for $\sigma_{22} + \sigma_{33} > 0$

$$\frac{(\sigma_{22} + \sigma_{33})^2}{Y_T^2} + \frac{\sigma_{23}^2 - \sigma_{22}\sigma_{33}}{S_{23}^2} + \frac{\sigma_{12}^2 + \sigma_{13}^2}{S_{12}^2} = \begin{cases} \geq 1 & \text{failure} \\ < 1 & \text{no failure} \end{cases} \tag{20}$$

Fourth, compressive matrix failure for $\sigma_{22} + \sigma_{33} < 0$

$$\left[\left(\frac{Y_C}{2S_{23}}\right)^2 - 1\right]\left(\frac{\sigma_{22} + \sigma_{33}}{Y_C}\right) + \frac{(\sigma_{22} + \sigma_{33})^2}{4S_{23}^2} + \frac{\sigma_{23}^2 - \sigma_{22}\sigma_{33}}{S_{23}^2} + \frac{\sigma_{12}^2 + \sigma_{13}^2}{S_{12}^2} = \begin{cases} \geq 1 & \text{failure} \\ < 1 & \text{no failure} \end{cases} \tag{21}$$

Fifth, inter-laminar tensile failure for $\sigma_{33} > 0$

$$\left(\frac{\sigma_{33}}{Z_T}\right)^2 = \begin{cases} \geq 1 & \text{failure} \\ < 1 & \text{no failure} \end{cases} \tag{22}$$

Sixth, inter-laminar compression failure for $\sigma_{33} < 0$

$$\left(\frac{\sigma_{33}}{Z_C}\right)^2 = \begin{cases} \geq 1 & \text{failure} \\ < 1 & \text{no failure} \end{cases} \tag{23}$$

where,

σij: denote the stress components and the tensile and compressive allowable strengths for lamina are denoted by subscripts T and C, respectively.

XT, YT, ZT: denotes the allowable tensile strengths in three respective material directions.

XC, YC, ZC: denotes the allowable compressive strengths in three respective material directions.

S12, S13 and S23: denote allowable shear strengths in the respective principal material directions.

RESULTS AND DISCUSSION

In order to conduct a failure simulation of the composite G1151/Resin epoxy, a simple coupon simulation test has been carried out, the present method was carried out by several authors [32-34]. The dimensions of the composite virtual coupon were 20 x10 x 1 mm, which represent a small volume of the material under uniaxial stress. The virtual coupon was discretized using different mesh densities.

The boundary conditions as presented in figure 7 was chosen as fixed from just one side and free from the others to simulate the tensile test. The mesh was chosen as Tri-mesh. A sensitivity analysis of the FE results was elaborated on different mesh size.

The composite specimen was continuously loaded in the fibre direction under displacement control to mimic a pseudo-static loading on the coupon (see Figure 7) Figure 8 shows the failure initiation results obtained at different mesh sensitivity.

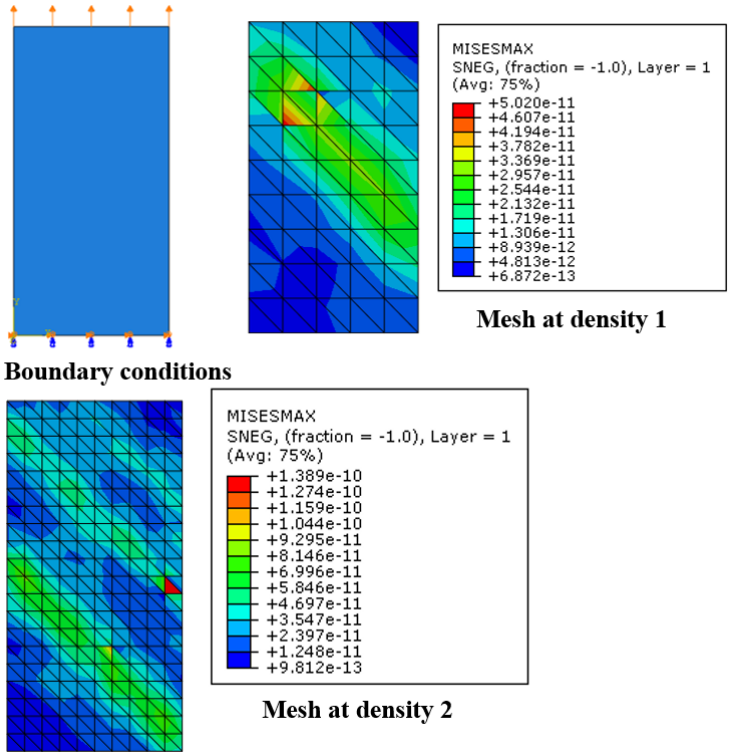

Figure 7. Von Mises results on G1151/Resin epoxy under bias tensile test and the mesh sensitivity study.

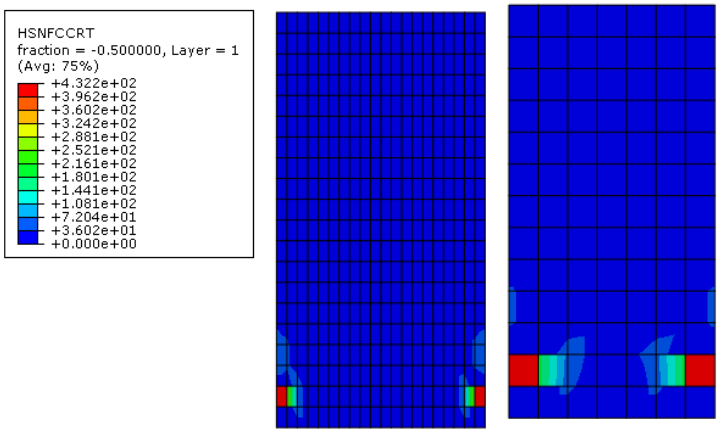

Figure 8. Failure localization on G1151/Resin epoxy under tensile test at 0°/90° for different mesh sensitivity.

The results obtained using different mesh types was elaborated in order to fix the appropriate mesh size for the FE simulation. The structural responses are almost identical ensuring the control of the energy dissipation regardless of mesh refinement and element topology. Minor differences may be attributed to rounding errors within the FE code. The Figure 8 shows the FE identification of the failure location; it was observed that the numerical predicted failure modes gives a good results comparing with the stress-strain response for tensile experimental findings on different specimen. This finding is similar to numerical and experimental results obtained by Donadon et al [20]. Moreover, the Figure 9 shows a comparison between experimental and simulated results for tensile test at 45°. The results present a similar maximum inclined displacement due to pre-orientation of yarns.

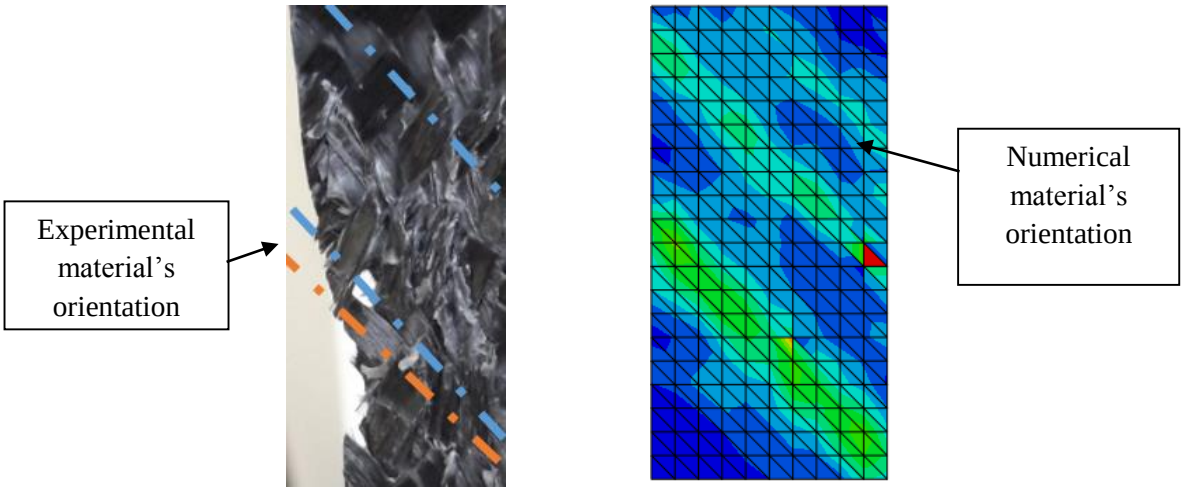

Figure 9. FE simulation vs experimental results of failure on G1151/Resin epoxy under bias tensile test (a) experimental result and (b) FE simulation.

CONCLUSIONS

In this work, the experimental characterization of composite G1151/Resin Epoxy was conducted in tension tests at 0°, 90° and 45°. The multiscale modelling of failure was elaborated in three main steps micro, meso and macro scale simulation. The microscale modelling approach was based on simulation of a 3D random RVE of a single yarn. Then it was selected an RVE for the whole woven fabric. The meso-scale simulation was developed in MATLAB in order to control the reorientation of yarns during application of forces to the whole composite structure. The meso simulation was developed based on the direction of loading (0°/90° or 45°). The macro FE simulation of failure based on the micro and meso modelling of the composite G1151/Resin Epoxy shows significant results in the way of identification of the failure contour of the material. The FE simulation versus experimental results of failure on G1151/Resin epoxy under tensile test gives a close result. It was concluded that the present failure prediction using a multiscale simulation approach could be implemented afterward in the prediction of failure during the deep drawing process of 2.5 D woven fabric composite.

ACKNOWLEDGEMENTS

The author would like to thank the University of Tabuk-KSA, University of Tunis-Tunisia and Art et Metiers Paris Tech Angers-France for laboratory, software facilities and supports.

REFERENCES

[1] Young K, David H. Allen, Ramesh R. Multiscale modeling and simulation of composite materials and structures. 2008.

[2] Schwab M, Todt M, Pettermann HE. A multiscale approach for modelling impact on woven composites under consideration of the fabric topology. Journal of Composite Materials. 2018;52: 2859–2874.

[3] Bassam ES, Federica D, Dmitry I, Stephen RH. An iterative multiscale modelling approach for nonlinear analysis of 3D composites. International Journal of Solids and Structures. 2018; 132–133: 42-58.

[4] Bassam ES, Dmitry I, Andrew CL, Stephen RH. Multi-scale modelling of strongly heterogeneous 3D composite structures using spatial Voronoi tessellation. Journal of the Mechanics and Physics of Solids. 2016; 88: 50-71.

[5] Durville D, Ganghoffer JF, Lomov S, Orgéas L., Kyriakides S. Multiscale modelling of fibrous and textile materials. International Journal of Solids and Structures. 2018; 154: 1-168.

[6] Abel C, Houman B. Numerical tools for composite woven fabric preforming. Advances in Materials Science and Engineering. 2013.

[7] Gherissi A, Abbassi F, Ammar A, Zghal A. Numerical and experimental investigations on deep drawing of G1151 carbon fiber woven composites. Appl. Compos. Mater. 2016; 23: 461–476.

[8] Naoki T, Yasutomo U, Yukio K, Masaru Z. Hierarchical modelling of textile composite materials and structures by the homogenization method. Modelling and Simulation in Materials Science and Engineering. 1999; 7: 207–231.

[9] András S, József UJ. Finite element modelling of the damage and failure in fiber reinforced composites. Periodica Polytechnica Mechanical Engineering. 2002; 46: 139–158.

[10] Okabe T, Nishikawa M, Toyoshima H. A periodic unit-cell simulation of fiber arrangement dependence on the transverse tensile failure in unidirectional carbon fiber reinforced composites. International Journal of Solids and Structures. 2011; 48:2948–2959.

[11] Hobbiebrunken T, Hojo M, Adachi T, Jong CD, Fiedler B. Evaluation of interfacial strength in CF/epoxies using FEM and in-situ experiments. Compos. A. 2006; 37:2248–2256.

[12] Gamesh S, Ramesh S, Mira M, Brian GF. Modelling matrix damage and fibre–matrix interfacial decohesion in composite laminates via a multi-fibre multi-layer representative volume element (M2RVE). International Journal of Solids and Structures. 2014; 51: 449-461.

[13] Green SD, Matveev MY, Long AC, Ivanov D, Hallett SR. Mechanical modelling of 3D woven composites considering realistic unit cell geometry. Composite Structures. 2014; 118:284–293.

[14] Kyle CW, Roberto A. Lopez-Anido, Senthil SV, Harun HB. Progressive failure analysis of three-dimensional woven carbon composites in single-bolt, double-shear bearing, Composites Part B. 2016; 84:266-276.

[15] Hashin Z. Failure criteria for unidirectional fiber composites. J. Appl. Mech. 1980; 47: 329-334.

[16] Matzenmiller A, Lubliner J, Taylor R. A constitutive model for anisotropic damage in fiber-composites. Mech. Mater. 1995;20.

[17] Abbassi F, Gherissi A, Zghal A, Mistou S, Alexis J. Micro-scale modeling of carbon-fiber reinforced thermoplastic materials. Applied Mechanics and Materials. 2012; 146:1-11.

[18] Paiva JMF, b, Mayer S, Rezende MC. Comparison of tensile strength of different carbon fabric reinforced epoxy composites. Materials Research. 2006; 9: 83-89.

[19] ASTM Standard D3039. Standard test method for tensile properties of polymer matrix composite materials. West Conshohocken, PA. ASTM International. 2002.

[20] Xiao X, Hua T, Li L, Wang J. Geometrical modeling of honeycomb woven fabric architecture. Textile Research Journal. 2015; 85:1651–1665.

[21] Kurbak A. Geometrical models for weft-knitted spacer fabrics. Textile Research Journal. 2017; 87:409–423.

[22] Kurbak A. Models for basic warp knitted fabrics Part III: the two guide bar fabrics (Double Tricot, Locknit, Reverse Locknit, Satin, Sharkskin). Textile Research Journal. 2019; 89: 1917–1937.

[23] ElAgamy N, Laliberté J. Historical development of geometrical modelling of textiles reinforcements for polymer composites: A review. Journal of Industrial Textiles. 2016; 45: 556–584.

[24] Zhu HX, Fan TX, Zhang D. Composite materials with enhanced dimensionless Young's modulus and desired Poisson's ratio. Scientific Reports 2015; 5.

[25] Akkerman R, de Vries RS. Thermomechanical properties of woven fabric composites. International Conference on Fibre Reinforced Composites FRC`98.1998:422-429.

[26] Giorgio I, Angew Z. Numerical identification procedure between a micro-Cauchy model and a macro-second gradient model for planar pantographic structures. Journal of Applied Mathematics and Physics. 2016; 67: 95.

[27] Dai S, Cunningham PR. Multi-scale damage modelling of 3D woven composites under uni-axial tension. Composite Structures. 2016; 142: 298–312.

[28] Zhai J, Zeng T, Xu G, Wang Z Cheng S, Fang D. A multi-scale finite element method for failure analysis of three-dimensional braided composite structures. Composites Part B: Engineering. 2017; 110 : 2017: 476-486.

[29] Kirane K, Salviato M, Bažant ZP. Microplane triad model for simple and accurate prediction of orthotropic elastic constants of woven fabric composites. Journal of Composite Materials. 2015; 50: 1247-1260.

[30] Döbrich O, Gereke T, Cherif C. Modeling the mechanical properties of textile-reinforced composites with a near micro-scale approach. Composite Structures. 2016; 135: 1-7.

[31] Fu X, Ricci S, Bisagni C. Multi-scale analysis and optimization of three-dimensional woven composite structures combining response surface method and genetic algorithms. CEAS Aeronaut J. 2017; 8:129–141.

[32] K. Supar and H. Ahmad. Multi-holes configurations of woven fabric kenaf composite plates: experimental works and 2-D modelling. Journal of Mechanical Engineering and Sciences. 2018; 12: 3539-3547.

[33] S. B. Rayhan. A comprehensive study on the buckling behaviour of woven composite plates with major aerospace cutouts under uniaxial loading. Journal of Mechanical Engineering and Sciences. 2019; 13: 4756-4776.

[34] S. D. Fanourgakis, D. E. Mazarakos, V. Kostopoulos. Fluid–structure interaction study for the DIFIS system's composite riser tube. Journal of Mechanical Engineering and Sciences. 2018; 12: 4243-4262.